Ocean and Coastal Management 259 (2024) 107454

Contents lists available at ScienceDirect

Ocean and Coastal Management

journal homepage: www.elsevier.com/locate/ocecoaman

Quantifying the impact of small boats on Posidonia seagrass meadows: Methods and path for future efficient management of anchoring pressure

Thomas Bockel [a,b,*], Noémie Bossut [e], Nicolas Mouquet [b,c], David Mouillot [b], Quentin Fontaine [d], Julie Deter [a,b]

[a] Andromède océanologie, 7 place Cassan, Carnon plage, 34130, Mauguio, France
[b] MARBEC, UMR IRD-CNRS-UM-IFREMER 9190, Université Montpellier, 34095, Montpellier Cedex, France
[c] FRB - CESAB, Institut Bouisson Bertrand. 5, rue de l'École de médecine, 34000, Montpellier, France
[d] STARESO, Pointe Revellata, BP33, 20260, Calvi, France
[e] LAMSADE, UMR CNRS 7243, Université Paris Dauphine-PSL, 75775, Paris, France

ARTICLE INFO

Keywords:
Seagrass
Pressure monitoring
Mooring
Small boats
Image analysis
Satellite
AIS

ABSTRACT

Coastal ecosystems are exposed to anthropogenic pressures worldwide. Seagrasses are sensitive to human activities, especially through physical stress. Among them, boats induce many pressures including physical degradation through anchoring. Mapping the anchoring pressure of large boats (≥24 m) can be done with traditional methods but is still challenging for smaller boats. Thus, the impact of large boats on coastal ecosystems is better documented and more efficiently regulated in comparison with small ones.

Here, we characterize the pressure and the impact of boats anchoring on *Posidonia oceanica* seagrass beds through the proxy of three landscape indices and compare anchoring surveillance methods.

We show that small boats also have an impact on *P. oceanica* when anchoring.

AIS (Automatic identification System) and low resolution satellite imagery are poorly adapted to detect small boat anchoring.

High resolution satellite imagery is a very efficient tool suitable even for small boats detection, but is for now limited to targeted surveys due to its high costs.

We propose an automatic detection/localization tool adapted to multisource imagery and test it successfully on a case study in Corsica (France).

Overall our study provides key quantified elements for the design of future efficient surveillance and management of anchoring pressure.

1. Introduction

Coastal ecosystems, including mangroves, near shore reef ecosystems and seagrass beds, are among the most important ecosystems not only ecologically, but also economically and socially (Martínez et al., 2007; Barbier et al., 2011). Those sensitive ecosystems are severely and increasingly threatened worldwide by human activities (Halpern et al., 2008, 2015) including shipping (Halpern et al., 2019), which is responsible for pollution and physical damage with anchoring (Deter et al., 2017).

Mapping anchoring pressure was traditionally performed by manual counts of boats, from a boat, from shore, on fixed camera images (Bonhomme et al., 2013; Schohn et al., 2019), or from airplanes during aerial survey (Holon et al., 2015; Serra-Sogas et al., 2021; MEDOBS, 2024).

Since 2004, the Automatic Identification System (AIS) device is mandatory on ships of 300 gross tonnage and upwards (IMO, 2018). This electronic transponder, communicating the ship position and characteristics to surrounding receiving stations, allowed huge progress in mapping large boats (≥24 m) anchoring events (Deter et al., 2017; Pergent-Martini et al., 2022; Bockel et al., 2023). AIS however does not effectively sample small boats (Serra-Sogas et al., 2021).

Other methods like Synthetic Aperture Radar (SAR) (Greidanus et al., 2017) or optical (Kanjir et al., 2018) satellite imagery combined with efficient image analysis software such as SUMO for SAR images, are also used to detect large boats (≥24 m) anchoring events. The ever

* Corresponding author. Andromède océanologie, 7 place Cassan, Carnon plage, 34130 Mauguio, France.
E-mail address: thomas.bockel@andromede-ocean.com (T. Bockel).

https://doi.org/10.1016/j.ocecoaman.2024.107454
Received 15 July 2024; Received in revised form 13 September 2024; Accepted 21 October 2024
Available online 2 November 2024

increasing resolution of satellite imagery has recently made it possible to achieve impressive performance in ship detection, even on small boats (Jialeng et al., 2023).

Smartphones and social networks are another huge source of image data (Toivonen et al., 2019) that could also potentially be useful to map anchoring pressure whatever the boat size.

Recent developments in Artificial Intelligence (AI) and especially deep learning (LeCun et al., 2015; Wu et al., 2020) already allowed massive improvements in detection and classification on satellite imagery (Goswami et al., 2020), with applications for boats monitoring (Kanjir et al., 2018; Patel et al., 2022; Paolo et al., 2024).

The Mediterranean sea is crossed by intense maritime traffic (March et al., 2021) and a mecca for pleasure craft (Carreño and Lloret, 2021). This implies considerable pressures for its great biological diversity, with more than 17,000 marine species and a very high rate of endemism (20–30 %) (Coll et al., 2010; UNEP/MAP, 2024). The endemic species *Posidonia oceanica* forms a protected key habitat hosting a high number of species and providing many services (Boudouresque et al., 2012). *P. oceanica* seagrass beds are very sensitive to anthropogenic threats (Boudouresque et al., 2009) and 70 % of its habitat is projected to be lost by 2050 (Intergovernmental Panel on Climate Change, 2022).

Large boat (≥24 m) anchoring highly impacts *Posidonia oceanica* meadows (Boudouresque et al., 2012; Deter et al., 2017; Pergent-Martini et al., 2022). Few existing local studies also suggest an impact from small boats (Francour et al., 1999; Milazzo et al., 2004; Rouanet et al., 2013), with varying results concerning its severity (Boudouresque et al., 2009). Anchoring impacts on *P. oceanica* meadows are traditionally characterized by large scars visible on aerial imagery for shallow depths (<10 m deep) and sonar imagery for deeper areas (Pasqualini et al., 1999) but can also be derived from patterns observed in landscape indices. The decline index (proportion of living meadow) and the patch cohesion index (characterizing the cohesion of the meadow) are the landscape indices describing the conservation status of the meadow that best correlated with anthropogenic pressures in the literature (Holon et al., 2018; Houngnandan et al., 2020). Their application to characterize the conservation status of Posidonia seagrass beds, coupled to a map of the anchoring pressure of large boats (≥24 m) (Deter et al., 2017), has led to a tightening of regulations in France (Deter et al., 2022), regulations which have effectively reduced these pressures in return (Bockel et al., 2023). Many questions now arise for smaller boats: where do they anchor? To what extent do they impact when anchoring? What methods are best suited to monitor the anchoring pressure of small boats?

The aim of this work was to address these questions. We first investigated the impact of large and small boat anchoring on the French *Posidonia oceanica* meadows using the proxies of landscape indices and AIS anchoring positions. We then compared AIS with the other traditional methods used to monitor anchoring pressure. We proposed a new detection and localization tool based on images from different sources and AI and tested it on a case study in Corsica. We finally showed the relevance of high-resolution satellite imagery for detecting small boats at anchor, and discussed the design of efficient anchoring surveillance.

2. Material and methods

2.1. Impact of boat anchoring on Posidonia oceanica meadows, using AIS

The study area for this analysis was the entire French Mediterranean sea. Details on the bathymetric range used in the analysis are provided below in section "1–3 Analysis".

2.1.1. Anchoring events and duration from AIS positions

AIS data were collected from two different sources. AIS data from 2010 to 2018 were collected from Marine traffic database (www.marinetraffic.com). Those AIS positions correspond to positions of declared anchoring activity, received by terrestrial AIS stations, with an hourly frequency. AIS data from 2019 to 2022 came from the terrestrial receiving stations of AIShub network (www.aishub.net) and from the vesselfinder database (www.vesselfinder.com). Those AIS data are raw positions that were collected with a frequency of one position every 2 min. All AIS data contain information on boat identification and size, time of detection, geographic coordinates, heading direction, speed, dimensions, type, and destination (when declared). All AIS positions were combined in a unique database independently of source or frequency.

The methodology used to obtain the anchoring positions from AIS (approx. 55,000 between 2010 and 2018 and approx. 160,000 between 2019 and 2022) was derived from the work of Deter et al. (2017) and Bockel et al. (2023). Briefly, a boat was considered at anchor when its successive AIS positions (at least four) had low speed (<1 kt) and were stationary (distance between points ≤600 m). A regression circle was then fitted on those positions to calculate the anchoring polygon.

The proportion of anchoring positions happening during the summer (July and August) was calculated.

Cumulated anchoring duration was calculated on 100 × 100 m cells for big boats (≥24 m) and small boats (<24 m) separately. For each boat size category, a pixel was labeled as "anchoring" if anchored only by boats belonging to the size category or smaller.

2.1.2. Landscape indices from the marine habitat map

Landscape indices were calculated for *Posidonia oceanica* (Houngnandan et al., 2020) based on the 2023 update of the 1/10,000 map of the marine habitat in the entire French Mediterranean sea between 0 and 80 m deep (Andromède océanologie, 2014) (www.medtrix.fr, donia expert project). Habitat data was rasterized at a resolution of 5 m before calculating the three following landscape indices: decline index, patch cohesion index and landscape division index. Formulas for each index were reported in Table S1. The landscape indices were calculated in 100 × 100 m cells using the R software 4.2.1 and the packages SDMTools 1.1–221.2 and terra 1.6–17.

2.1.3. Analysis

Values of each landscape index were calculated and plotted on areas with and without small or large boat anchoring and the differences were tested using a Wilcoxon test. Very shallow areas (<5 m deep) and the deepest areas (>30 m deep) were removed from this analysis, to avoid landscape patterns outside of the anchoring bathymetric range influencing the results.

2.2. Comparison of AIS and other traditional methods used to map anchoring

This analysis was realized on a study area covering the Medobs and Sentinel 1 SAR acquisition areas in the French Mediterranean sea within a period covering the summer of 2020. Areas and dates of acquisitions for Medobs, AIS and Sentinel 1 SAR are reported in Fig. S1 and Table S2.

2.2.1. AIS

AIS-derived anchoring events were mapped as described above.

2.2.2. Sentinel 1 SAR images and SUMO

Sentinel 1 SAR images were downloaded from NASA EARTHDATA ASF data platform (search.asf.alaska.edu). L1 Detected High-Res Single-Pol (GRD-HS) sentinel products were used. Sentinel 1 images (n = 13) were analyzed using the Search for Unidentified Maritime Objects (SUMO) software (Greidanus et al., 2017). Cross-polarization and co-polarization detection threshold adjustments were applied based on the literature (Galdelli et al., 2021; Pita et al., 2022). No land buffer was used. Coordinates and estimated size of each detected boat were obtained.

2.2.3. Medobs

Medobs (MEDOBS, 2024) is a monitoring network of human activities using aerial surveillance on the French Mediterranean coast. Operated by the Air Attack Technologies company and funded by the Agence de l'eau Rhône Méditerranée Corse (French water agency), this network includes multiple aerial surveys of the entire coastline including Corsica, with a higher density of flights during summer. Boats are manually counted and regrouped by anchoring zones (hotspots of anchoring) and size classes (<10 m: small; 10–24 m: medium; ≥24 m: large). Thirteen survey dates and 1068 anchoring zones were analyzed for the 2020 summer.

2.2.4. Analysis

For each Medobs anchoring zone, the number of boats detected by Medobs and by AIS/SAR were compared. In order to filter out zones out of AIS/SAR detection ranges, only Medobs anchoring zones containing AIS detections/SAR detections were kept for this analysis. Sentinel 1 SAR images were acquired by the satellite at two different timeframes: 5 a.m. or 5 p.m. Boat detections on 5 a.m. images were considered as boats anchored since the day before the detection. The mean percentages of "medobs boats" detected by AIS and SAR for each size class were calculated. The difference of detection performance between size classes and detection methods were tested using a Wilcoxon test.

2.3. Terrestrial and aerial imagery to better map anchoring boats

A suite of tools was developed to detect any type and size of boats on multisource imagery, and to localize their position based on the metadata of the images.

2.3.1. Images dataset

The dataset of images (344 images) was composed of two main types of images (Fig. S2). The first type of images (71 % of the images) is multisource images: smartphones and drones images taken by our team (Andromède océanologie) during the summer in 2022 and 2023, fixed camera on the coast (Stareso, summer 2020) and aerial images (Medobs, summer 2022). The second type of images (29 % of the images) were downloaded from an opensource boats images dataset (Bogue Sound Team Roboflow, 2023).

All images were randomly separated between training set (83 %), test set (7 %) and validation set (10 %). Labeling of boats on images before training was performed with the online application Make Sense (Skalski, 2019) and was semi supervised (all images were pretreated with YOLOv5 and then checked visually and corrected manually when needed).

2.3.2. YOLOv8 detection algorithm and its improvement

The boat detection algorithm was trained using YOLOv8 on a GPU equipped server. Although initially planned with 500 epochs (an "epoch" refers to one complete cycle through the entire training dataset) to ensure comprehensive learning, the training was concluded after approximately 300 epochs due to satisfactory performance metrics achieved earlier than expected. This early stopping helps prevent overfitting while maintaining high accuracy. Images were automatically resized to a standard size of 640 by 640 pixels to facilitate uniform processing.

2.3.3. Localization methodology

The developed localization tool was entirely based on the metadata of the image. Image metadata are encrypted in image files in Exif format (Exchangeable Image File Format). They contain information on the image shot, essential for localization: date, coordinates, altitude, camera captor width and focal length, angles of the shot (pitch, yaw and roll), and image height and width (in pixels). Some devices such as drones contained very complete image metadata, but others such as smartphones contained metadata of variable quality, often lacking several parameters. In this case, precise localization was only possible when the photographer manually provided missing parameters, at least date, coordinates of the camera and yaw angle. Camera captor width and focal length could be inferred from the camera model, roll was assumed to be 0 (the localization tool doesn't work otherwise), altitude could be inferred from the coordinates and freely accessible digital elevation models, and pitch was assumed to be linearly linked to the height of the relative horizon in the image (pitch of 0 for a relative horizon of 0.5 and pitch of −30° for a relative horizon of 1) using the following formula: pitch (p) = (−60 * relative horizon) - 30.

Using basic principles of trigonometry (Fig. 1), the boat real position was then derived from its relative position in the image (rel_x and rel_y, defined at the middle bottom of the detection bounding box) using the following equations (all terms in the equations are shown and defined in Fig. 1):

$$phiXh = atan((Sh * (abs(rel\_x) * 2)) \ / \ Cf \ / \ 2)$$

$$phiYh = atan\left(\left(Sh * (image\,height \ / \ image\,width) * \left(abs\left(rel\_y\right) * 2\right)\right) / \ Cf \ / \ 2\right)$$

if boat on top half of image (y *coordinate in image* < 0.5):

$$K = A \ / \ (tan(-p) - phiYh)$$

if boat on bottom half of image:

$$K = A \ / \ (tan(-p) + phiYh)$$

$$R = sqrt\left(A^2 + K^2\right)$$

if boat on right half of image (x *coordinate in image* > 0.5):

$$W = R * tan(phiXh)$$

if boat on left half of image:

$$W = -(R * tan(phiXh))$$

$$x = X + W * cos(dir) + K * sin(dir)$$

$$y = Y - W * sin(dir) + K * cos(dir)$$

A filter was then applied to consider the low reliability of localization near the edges of the image or near the relative horizon. Only boats detected in the 99 % of the image farthest from the image edges (or from the relative horizon when shot not vertical and altitude <10 m) were kept.

2.3.4. Performance analysis of detection and sensitivity analysis of localization

The performance of the detection model was evaluated by calculating its average precision (proportion of true positive detections among all positive detections) and recall (proportion of true positive detections among all actual positive ones) and by comparing between the YOLOv8 standard algorithm using default YOLO coco weights, and our YOLOv8 custom algorithm trained on our images dataset.

The performance of the localization tool was evaluated by running a sensitivity analysis on a separate subset of images where the true location of the detected boat was known. The error between the true position and the estimated position was calculated. Each factor potentially influencing this localization error was extracted from the images: distance between boat and camera, altitude, method of acquisition (smartphone or drone), relative position of the boat with respect to the horizon on the image, relative position of the boat with respect to the center of the image, and relative position of the horizon. A linear regression was performed to assess the relationship between each factor and the localization error (previously log-transformed for normality).

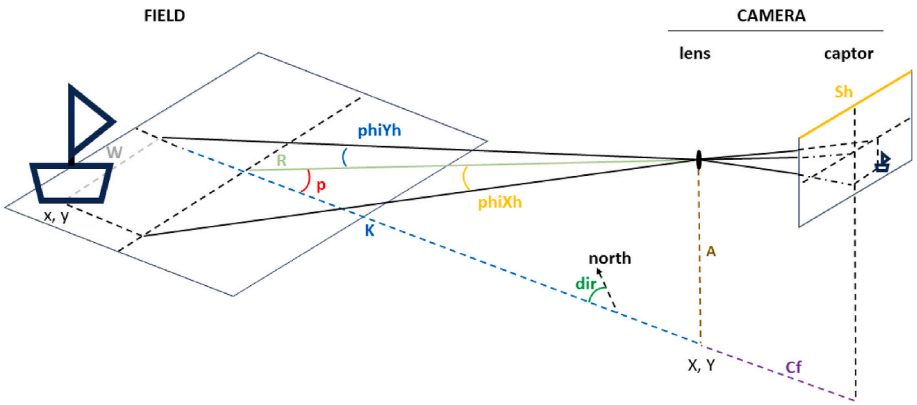

Fig. 1. Schematic view of localization method. Boat position on the field (left) is derived from boat position on the camera image (right), using camera metadata (captor width Sh and focal length Cf) and field metadata (altitude A and coordinates X and Y of the camera, angles of the shot (dir and p), and distance K to the target.

2.3.5. Application of the custom YOLO detection and localization methodology to the case study of the alga bay

The "Alga" bay, located north of the city of Calvi in Corsica (France) (Fig. S3), was equipped with a Bushnell 30 MP CORE Trail Camera, positioned at an altitude of 89 m in order to cover the entire bay. Photographs were acquired every hour during daylight for the summer period of 2020. The first exploitable image every morning (8 a.m.) was considered the most representative of the boats anchored during the night and extracted from the database. Those images (n = 62) were then processed through our custom detection localization algorithm (Figure S3, Figure S4). The depth category was extracted for each detection using a bathymetric raster produced by combining the best available resolution between SHOM data, and Andromède océanologie bathymetric dataset; categories were defined as follows: deeper than 20 m, 20 to 10 m, and shallower than 10 m. The average number of boats detected per night and depth category was calculated and compared with anchoring boats detected during the same night based on AIS data using the method described above. The difference between both methods was tested using a Wilcoxon test.

2.4. High resolution optical satellite imagery to better map anchoring boats

A pre-trained YOLOv8 detection algorithm was tested on high resolution optical satellite imagery to detect small boats at anchor.

2.4.1. Images and pretreatment

The images used were Airbus Pleiades multispectral (2 m resolution) and panchromatic (50 cm resolution) on a study area of 17 km width and 13 km height centered on the area of Bonifacio and the Lavezzi islands in south Corsica (Fig. S5). Images were available at three timestamps: 2023/07/19 at 10:31 a.m., 2023/07/26 at 10:28 a.m., and 2023/08/14 at 10:31 a.m. The 2023/07/26 image was removed from the analysis because the numerous waves negatively affected the YOLO detection performances.

Images were pansharpened and tilled at a size of 1000 by 1000 pixels using gdal 3.0.4. An overlap of 100 pixels was used during tiling in order not to remove any boats from the database. Tiles containing shallow water areas (0–20 m deep) were extracted for boats detection.

2.4.2. YOLO detection and validation

YOLOv8 base weights were obtained from a pre-training performed on a google earth dataset (Cole, 2023). Boats detection was performed on each previously created tile using YOLOv8 and the obtained base weights, with an automatic resizing of the tiles to a standard size of 640 by 640 pixels (Fig. S6). A sample of 100 tiles per image, with the associated detections, was then used to create a reference annotation dataset using Roboflow (Dwyer et al., 2024) online annotation tool (774 boats annotated for the 2023/08/14 image and 670 boats annotated for the 2023/07/19 image). YOLOv8 algorithm using base weights was then retrained using the 2023/07/19 reference dataset as training set, and 2023/08/14 reference dataset as validation set. Boat detections on land or inside ports were filtered out. Precision and recall metrics were then calculated for each boat size class (0–5m, 5–10m, 10–15m, >15m).

3. Results

3.1. Impact of boat anchoring using AIS

The anchoring dataset contained 225470 anchoring polygons between 2010 and 2022 (129552 for large boats (≥24 m) and 95918 for small boats (<24 m)). Most anchoring events (57 %) happened during the summer (July and August). Cumulated anchoring duration calculation gave a total of 23092 100 m × 100 m cells with anchoring (11235 containing anchoring of only large boats and 3389 containing anchoring of only small boats).

The decline index was significantly higher on areas with large boat anchoring compared to areas without large boat anchoring ($W = 2.5\ 10^8$, $p < 0.001$, $n = 85114$), and not significantly different between areas with or without small boat anchoring ($W = 8.9\ 10^7$, $p > 0.1$, $n = 78932$) (Fig. 2).

The patch cohesion index was significantly lower on areas with anchoring compared to areas without anchoring; for large boats ($W = 2.8\ 10^8$, $p < 0.001$, $n = 81573$), and for small boats ($W = 1.1\ 10^8$, $p < 0.001$, $n = 75464$) (Fig. 2).

The landscape division index was significantly higher on areas with anchoring compared to areas without anchoring; for large boats ($W = 2.5\ 10^8$, $p < 0.001$, $n = 81573$), and for small boats ($W = 5.5\ 10^7$, $p < 0.001$, $n = 75464$) (Fig. 2).

3.2. Comparison of AIS and other traditional methods used to map anchoring

Differences between size classes, for both detection methods, were significant only between large (≥24 m) and small boats (<10 m) (AIS: $W = 1.1\ 10^3$, $p < 0.001$, $n = 313$; SAR: $W = 9.6\ 10^2$, $p < 0.001$, $n = 83$) and between medium (10–24 m) and small boats (AIS: $W = 5.2\ 10^4$, $p < 0.001$, $n = 498$; SAR: $W = 2.4\ 10^3$, $p < 0.001$, $n = 118$) with larger boats being more detected than small ones (Fig. 3). Differences between detection methods were significant only for medium boats ($W = 9.7\ 10^3$, $p < 0.001$, $n = 304$) with more boats detected on average by AIS (28 % of Medobs observations) than by SAR (12 %) (Fig. 3).

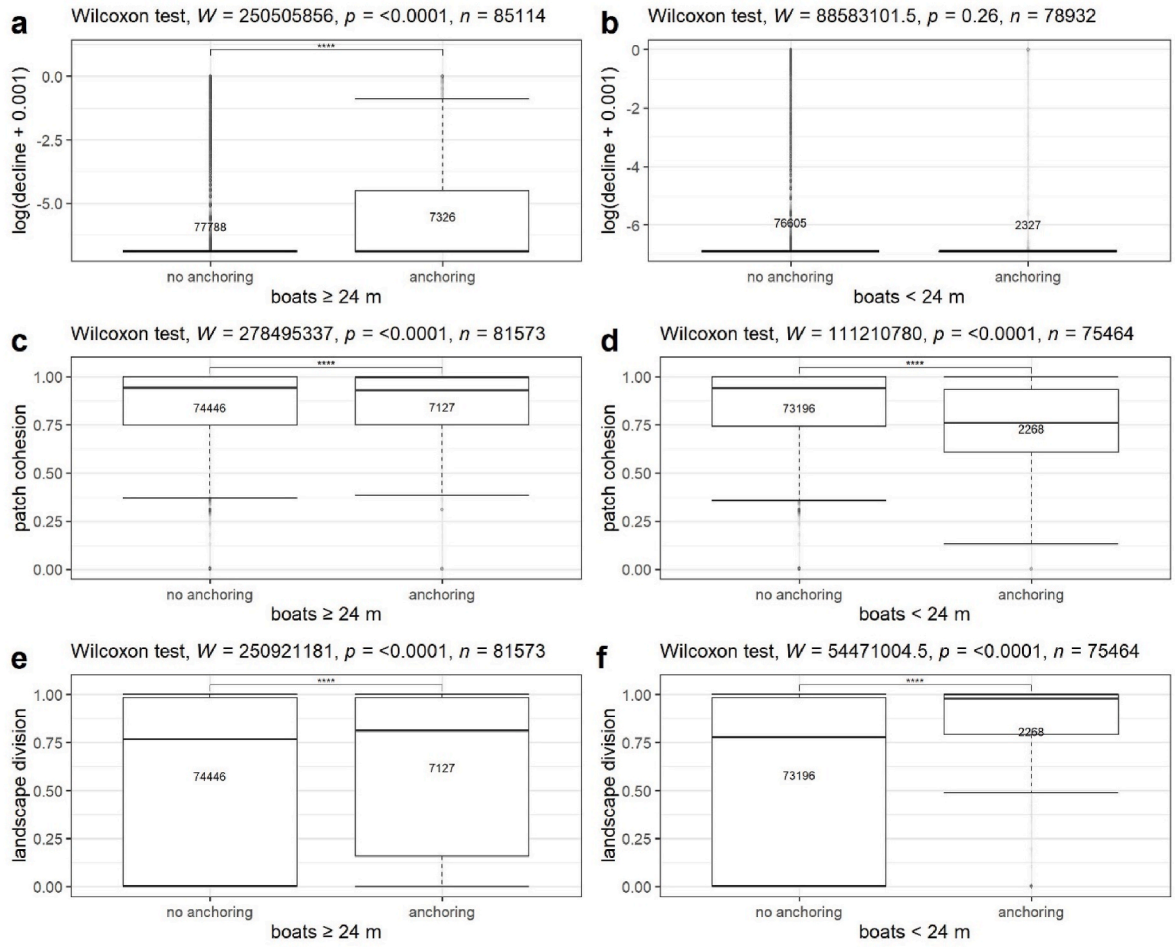

Fig. 2. Statistical distribution of landscape indices for each size category of ais boats (≥24 m or < 24 m) with or without anchoring. a. log(decline index) (boats ≥24 m), b. log(decline index) (boats <24 m), c. patch cohesion index (boats ≥24 m), d. patch cohesion index (boats <24 m), e. landscape division index (boats ≥24 m), f. landscape dvision index (boats <24 m). Numbers inside the bars indicate the number of 100 × 100 m cells where each indicator was calculated (this number is higher for the decline index compared to the other indices because also taking into account dead matte).

3.3. Terrestrial and aerial imagery to better map anchoring boats

3.3.1. Performances of the detection algorithm and improved model

On the validation dataset, YOLOv8 showed an average precision of 0.63 and an average recall of 0.42. The improved custom model showed an average precision of 0.81 and an average recall of 0.69. The custom model presents a good balance between precision and recall (Fig. 4, Fig. S7).

3.3.2. Localization performances and sensitivity analysis

The linear regression between the images metadata and the logarithm of the localization error explained 73 % of the variance of the localization error ($F = 51$, $p < 0.001$, adjusted $R^2 = 0.73$). The localization error was significantly negatively influenced by altitude ($t = -3.8$, $p < 0.001$) and significantly positively influenced by the method ($t = 2.2$, $p < 0.05$) and the distance between the boat and the camera ($t = 10$, $p < 0.001$). The average localization error under ideal conditions (using the drone method with a distance between the boat and the camera below 200 m) was 16 m (Table S3 and Fig. 5).

3.3.3. Application of the YOLO detection and localization methodology to the case study of the alga bay (Corsica)

The average number of detected anchored boats per night and detection method was equal to 0.032 (AIS) and 0.05 (images) deeper than 20 m; 1.6 (AIS) and 1.8 (images) between 10 m and 20 m deep; and 2.7 (AIS) and 10 (images) shallower than 10 m (Fig. 6). The average number of anchored boats detected per night increased significantly with decreasing depth, for both methods ($W < 1221$, $p < 0.001$ $n = 62$). The number of anchored boats detected per night was significantly higher for images than AIS at a shallow depth (<10 m) ($W = 240$, $p < 0.001$, $n = 62$). The differences between images and AIS were not significant for the other depth categories (10–20m: $W = 1669$, $p > 0.1$, $n = 62$; +20m: $W = 1891$, $p > 0.1$, $n = 62$) (Fig. 6) (see Fig. 7).

3.4. High resolution optical satellite imagery to better map anchoring boats

Post-training of YOLOv8 base algorithm using 2023/07/19 training dataset did not improve the performance of the detection algorithm on the 2023/08/14 validation dataset. Average precision on the validation dataset was equal to 0.91, and average recall was equal to 0.77. Precision vs recall, precision vs confidence and recall vs confidence curves were reported in Fig. S8. After filtering out detections on land and inside ports, average precision values per size class were equal to 0.5 (0–5m), 0.87 (5–10m), 0.91 (10–15m), 0.88 (>15m), and average recall values per size class were equal to 0.75 (0–5m), 0.69 (5–10m), 0.76 (10–15m), 0.84 (>15m).

While recall values were relatively high and constant for each boat size class, precision value was 43 % lower for boats smaller than 5 m compared to boats longer than 5 m. This value is to be interpreted with caution as only four boats smaller than 5 m were present in the dataset.

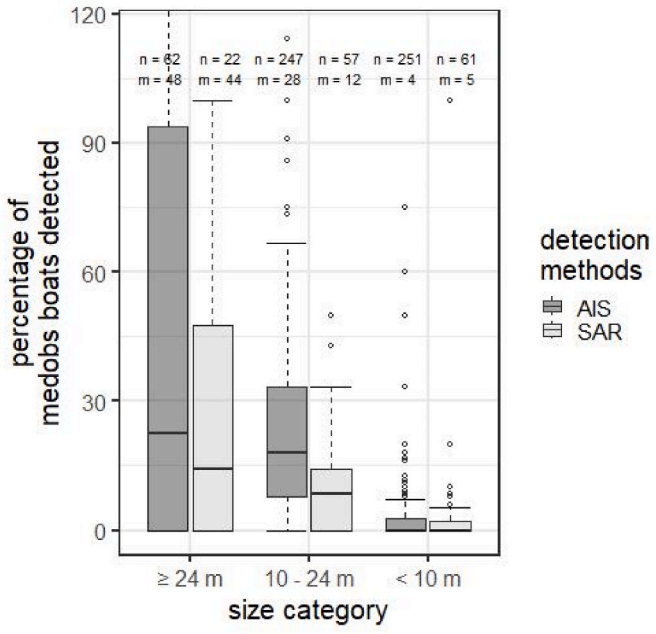

Fig. 3. *Mean percentage of Medobs boats detected by AIS and SAR, for each size category (≥24 m, 10–24 m, <10 m; n = number of Medobs anchoring zones, m = mean percentage of Medobs boats detected).*

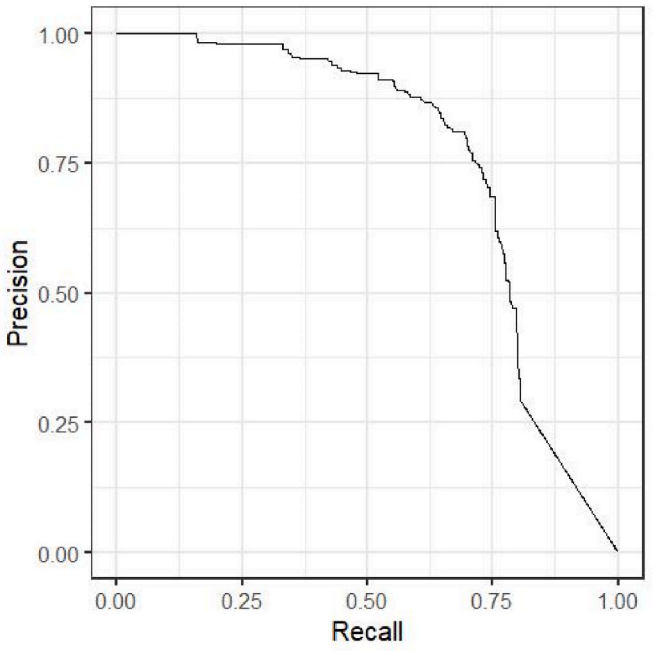

Fig. 4. Precision recall curve for the custom detection model.

4. Discussion

4.1. Impact of boat anchoring using AIS

The impact of large boats (≥24m) anchoring was confirmed on each analyzed landscape indices (decline, patch cohesion and landscape division) for *Posidonia oceanica* meadows. Moreover, small boats detected by AIS (<24 m) are also responsible for measurable impacts: patch cohesion index and landscape division index were significatively degraded in presence of small boats anchoring. Small boats damage the spatial configuration of the meadows when anchoring, and these

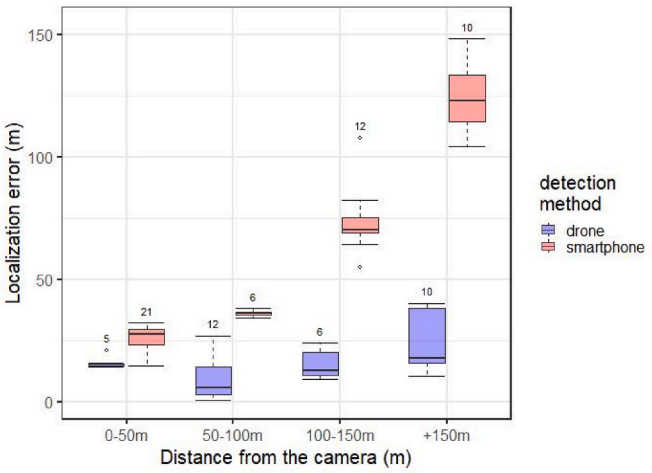

Fig. 5. Error of the localization method as a function of the distance to the camera and the acquisition method (drone or smartphone). The number of images is indicated above each boxplot.

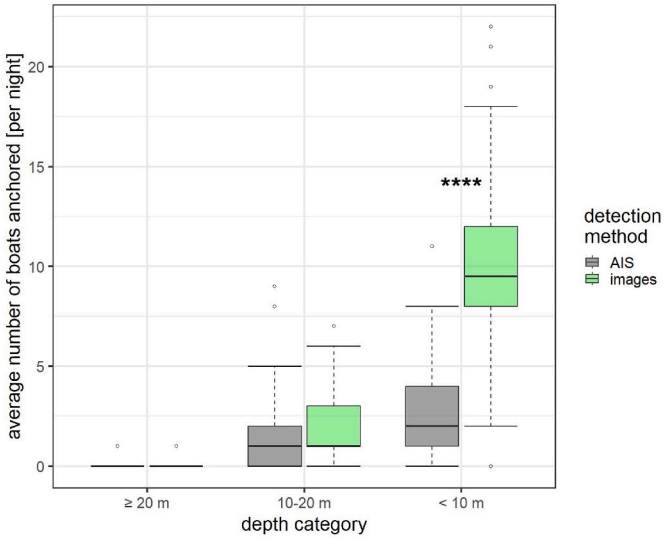

Fig. 6. Average number of boats detected at anchoring per night, for each depth category and detection method.

changes in configuration could be an early warning of future decline, not yet detected. Scars induced by small boats anchoring in the meadow could also be too narrow to be detected as dead matte during lateral sonar acquisitions, explaining the absence of significant impact on the decline index.

The impact of small boats is detected even though their number is underestimated due to the rare presence of AIS equipment on small boats (Greidanus et al., 2017; Paolo et al., 2024) (as shown in section 2 "Comparison of AIS and other traditional methods used to map anchoring"). It is therefore necessary to monitor those anchoring events, whether or not the boats are equipped with AIS, because they are not currently affected by the French regulation prohibiting anchoring in *P. oceanica* seagrass beds. This more detailed knowledge depending on the size is all the more important as the number of boats, including small boats, continues to increase, particularly in protected marine areas, and requires monitoring to address carrying capacity issues (Gómez et al., 2023).

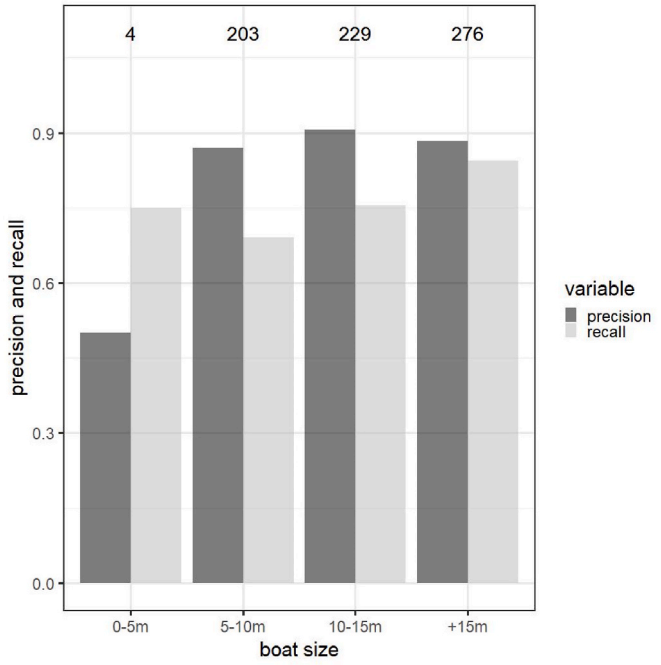

Fig. 7. Precision and recall metrics per size class of YOLOv8 algorithm on optical satellite imagery. Numbers at the top indicate the number of boats per size class.

4.2. From the comparison of AIS and other traditional methods to the test of terrestrial and aerial imagery to better map anchoring boats

This study demonstrated both at the scale of the French Mediterranean sea and at the scale of a bay, that AIS data, while allowing to detect a general pattern of impact, are poorly adapted to a detailed mapping of small boats anchoring impacts, in accordance with the literature (Serra-Sogas et al., 2021).

Similarly, freely available low resolution (10 m) SAR satellite imagery was shown to be poorly adapted to detect small boats (only 12 % of small Medobs boats (10–24 m) and 5 % of very small boats (<10 m) detected on SAR S1 images during summer 2020), in accordance with the literature (Greidanus et al., 2017).

As Medobs images cannot be acquired continuously and automatically, alternative methods must be proposed. Using multi-source images, the image-based tool developed in this work showed very good detection (average precision of 0.81 and average recall of 0.69) and localization (average localization error of 16 m under ideal conditions) performances. Some limitations must however be kept in mind under certain conditions such as very low altitude (below 2 m) and/or large distance to targets (above 2 km) and the presence of detection artefacts (important sun reflections at the sea surface, presence of buoys). Most of these limitations can however be controlled when using fixed cameras with well known acquisition metadata (see below).

The case study of the Alga bay showed a very similar rate of detection by AIS and the camera for areas deeper than −10 m but many anchoring were missed by AIS compared to the camera for areas shallower than −10 m. These anchoring events at such shallow depths most probably correspond to the smallest boats. The absence of an estimation of the boat size is a limitation of the image-based method, but this information could be calculated if the wind conditions are known at the date of acquisition of the image, and if the camera line of sight is perpendicular to the dominant wind in the area. The camera should be placed at a minimal altitude of approximately 5 m in order to obtain an acceptable localization error for boats as far as approximately 1 km from the camera. The automatic camera detection localization tool is moreover flexible and adapted to any source of terrestrial or aerial imagery (smartphone, drone, small aircraft such as ultra-light motorized planes (ULMs), or even webcams or social networks images), and provides automatic boat detection and localization, allowing important time gains in data analysis. The image acquisition represents a very low cost (approximately 400 euros for the purchase, installation and usage of the camera).

This method is therefore perfectly adapted to implement high-frequency surveillance on localized high-stake anchoring areas, and allows a detailed spatio-temporal reporting of large and small boats anchoring pressure, as well as an estimation of the total frequentation and turnover of boats on the surveyed sites. A project proposition has been designed with the local managers of the Agde Marine Protected Area (France) and the automatic camera detection localization tool should therefore be implemented there in 2025 if funded.

4.3. High resolution satellite optical imagery to better map anchoring boats

The YOLO detection algorithm tested in this work on Pleiades images showed very good performances (average precision of 0.91 and average recall of 0.77), close to the performances of the pretraining reference work (precision of 0.94 and recall of 0.93) (Cole, 2023), and very good compared to other recent studies (accuracy of 0.94 and precision of 0.74 (Jialeng et al., 2023), and accuracy of 0.99 and precision of 0.84 (Patel et al., 2022)). While recall values were relatively high and constant, precision appeared to decrease by more than 40 % for boats smaller than 5 m. This pattern could indicate a good reliability of the detection algorithm only for boats longer than 5 m, but is to be interpreted with caution as only four boats smaller than 5 m were present in the dataset. Waves, small private swimming pools, and very high density of boats next to each other (ports) were visually observed as factors negatively influencing the detection algorithm performances. Those factors can however easily be filtered out during images pre-selection and detections post-treatment. Besides, spatial data on existing mooring buoys is necessary to avoid false anchoring detections. Anchoring positions are moreover simplified as being the same as boat position. Real anchor position could however be derived assuming standard anchoring conventions and access to meteorological data (Forrester, 2020).

Satellite imagery field is evolving very fast and higher resolution (e.g. Pleiades neo (30 cm resolution) for optical imagery (Soubirane, 2019)) is already available. High resolution satellite imagery, as well as aerial surveys, are very appropriate for punctual monitoring to get a rough idea of the pressure, but their important costs make those methods less appropriate for regular surveillance.

5. Conclusion and future path for management

This work confirmed the impact of large boats (≥24 m) anchoring on *Posidonia oceanica* meadows using three different landscape indices (decline, patch cohesion and landscape division), and showed that small boats (<24 m) anchoring, despite very low accuracy detection by AIS, also seem to have an impact on *P. oceanica* meadows (impact detected on two of three analyzed indices: patch cohesion and landscape division). This work demonstrated that traditional monitoring methods such as AIS and low resolution freely available SAR satellite images, while detecting a reasonable part of large boats (≥24 m, approximately 50 %) are poorly adapted to small (10–24 m, approximately 20 %) and very small boats (<10 m, approximately 5 %) detection.

The strong suitability of high-resolution satellite imagery for small boats automatic detection was demonstrated but must be reserved, for the time, for punctual monitoring because of the relatively high costs involved. This work then proposed an automatic detection localization tool based on multi-sources images, and tested it successfully on a case study in Corsica. This tool is particularly adapted to high-frequency localized monitoring and could be easily deployed by harbourmasters and marine areas managers that could make appropriate use of existing

images or set up an automatic image-taking system. Combined to an automatic and connected image acquisition system, this tool could indeed be used in real time with applications such as the control of the frequentation with regard to anchoring areas carrying capacity. A real time application should be implemented on the field in France in 2025. With constantly improving technologies, it can be a struggle for managers to balance the pros and cons of each monitoring solution. The perfect solution does not exist, and addressing managers specific needs will inevitably involve a mix between the previously mentioned solutions. Well-designed monitoring and surveillance plans will both allow the construction of adapted management plans and enable managers to control and evaluate their efficiency. This work provides key quantified elements for the design of future efficient surveillance and management of anchoring pressure.

CRediT authorship contribution statement

Thomas Bockel: Writing – original draft, Methodology, Formal analysis, Data curation, Conceptualization. **Noémie Bossut:** Formal analysis, Data curation. **Nicolas Mouquet:** Writing – review & editing, Validation, Supervision, Conceptualization. **David Mouillot:** Formal analysis. **Quentin Fontaine:** Data curation. **Julie Deter:** Writing – review & editing, Validation, Supervision, Conceptualization.

Funding

This work is part of Thomas Bockel's Phd work funded by Agence Nationale pour la Recherche (ANR), the program "France Relance" and Andromède océanologie (convention ANR-21-PRRD-0102-01) in collaboration with UMR MARBEC and Université de Montpellier (research collaboration contract n° 211672).

Part of the data acquisition (camera images from the alga bay) were funded by Stareso, Collectivité de Corse and Agence de l'eau Rhône Méditerranée Corse as part of the STARECAPMED project.

Declaration of competing interest

The commercial affiliation to Andromède Océanologie of several authors (TB and JD) does not create any conflict of interest.

Acknowledgements

The authors would like to thank all participants to data acquisition and/or analysis, in particular Pierre Boissery from Agence de l'eau Rhône Méditerranée Corse and the Air Attack company for providing data from the Medobs campaigns, Ignacio Pita from Marbec research unit for his precious advices on the proper usage of SUMO, Thibault Catry from IRD for his help in obtaining Pleiades images, and all the staff and interns at Andromède Océanologie for their help.

Appendix A. Supplementary data

Supplementary data to this article can be found online at https://doi.org/10.1016/j.ocecoaman.2024.107454.

Data availability

Data will be made available on request.

References

Andromède océanologie, 2014. Les dessous de la mer méditerranée—Cartographie de la méditerranée française au 1/10000ème. Publi int Agence de l'eau RMC., 2014

Barbier, E.B., Hacker, S.D., Kennedy, C., et al., 2011. The value of estuarine and coastal ecosystem services. Ecol. Monogr. 81, 169–193. https://doi.org/10.1890/10-1510.1.

Bockel, T., Marre, G., Delaruelle, G., et al., 2023. Anchoring pressure and the effectiveness of new management measures quantified using AIS data and a mobile application. Mar. Pollut. Bull. 195, 115511. https://doi.org/10.1016/j.marpolbul.2023.115511.

Bogue Sound Team Roboflow, 2023. BogueSound_BoatDetection dataset. In: Roboflow. https://universe.roboflow.com/bogue-sound-team-roboflow/boguesound_boatdetection. (Accessed 7 February 2024).

Bonhomme, P., Bonhomme, D., Frachon, N., 2013. A METHOD for assessing anchoring pressure. Rapp. Comm. int. Mer Médit. 40, 2013.

Boudouresque, Bernard, Bonhomme, et al., 2012. Protection and Conservation of Posidonia Oceanica Meadows. RAMOGE - RAC/SPA.

Boudouresque, C.F., Bernard, G., Pergent, G., et al., 2009. Regression of Mediterranean Seagrasses Caused by Natural Processes and Anthropogenic Disturbances and Stress: a Critical Review, vol. 52, pp. 395–418. https://doi.org/10.1515/BOT.2009.057.

Carreño, A., Lloret, J., 2021. Environmental impacts of increasing leisure boating activity in Mediterranean coastal waters. Ocean Coast Manag. 209, 105693. https://doi.org/10.1016/j.ocecoaman.2021.105693.

Cole, Robin, 2023. Kaggle Ships in Satellite Imagery with YOLOv8. GitHub repository. https://github.com/robmarkcole/kaggle-ships-in-satellite-imagery-with-YOLOv8.

Coll, M., Piroddi, C., Steenbeek, J., et al., 2010. The biodiversity of the Mediterranean sea: estimates, patterns, and threats. PLoS One 5, e11842. https://doi.org/10.1371/journal.pone.0011842.

Deter, J., Bockel, T., Delaruelle, G., et al., 2022. Préservation des posidonies: les ressorts d'une collaboration efficace. In: sfecologie.org. https://sfecologie.org/regard/r104-juin-2022-j-deter-et-al-posidonies/. (Accessed 10 December 2022).

Deter, J., Lozupone, X., Inacio, A., et al., 2017. Boat anchoring pressure on coastal seabed: quantification and bias estimation using AIS data. Mar. Pollut. Bull. 123, 175–181. https://doi.org/10.1016/j.marpolbul.2017.08.065.

Dwyer, B., Nelson, J., Hansen, T., et al., 2024. Roboflow.

Forrester, G.E., 2020. The influence of boat moorings on anchoring and potential anchor damage to coral reefs. Ocean Coast Manag. 198, 105354. https://doi.org/10.1016/j.ocecoaman.2020.105354.

Francour, P., Ganteaume, A., Poulain, M., 1999. Effects of boat anchoring in Posidonia oceanica seagrass beds in the port-cros national park (north-western Mediterranean sea). Aquat. Conserv. Mar. Freshw. Ecosyst. 9, 391–400. https://doi.org/10.1002/(SICI)1099-0755(199907/08)9:43.0.CO;2-8.

Galdelli, A., Mancini, A., Ferrà, C., Tassetti, A.N., 2021. A synergic integration of AIS data and SAR imagery to monitor fisheries and detect suspicious activities. Sensors 21, 2756. https://doi.org/10.3390/s21082756.

Gómez, A.G., Balaguer, P., Fernández-Mora, À., Tintoré, J., 2023. Mapping the nautical carrying capacity of anchoring areas of the Balearic Islands' coast. Mar. Pol. 155, 105775. https://doi.org/10.1016/j.marpol.2023.105775.

Goswami, N., Kathiriya, K., Yadav, S., et al., 2020. Satellite imagery classification with deep learning : a survey. International Journal of Scientific Research in Computer Science, Engineering and Information Technology 36–46. https://doi.org/10.32628/CSEIT2065124.

Greidanus, H., Alvarez, M., Santamaria, C., et al., 2017. The SUMO ship detector algorithm for satellite radar images. Rem. Sens. 9, 246. https://doi.org/10.3390/rs9030246.

Halpern, B.S., Frazier, M., Afflerbach, J., et al., 2019. Recent pace of change in human impact on the world's ocean. Sci. Rep. 9, 11609. https://doi.org/10.1038/s41598-019-47201-9.

Halpern, B.S., Frazier, M., Potapenko, J., et al., 2015. Spatial and temporal changes in cumulative human impacts on the world's ocean. Nat. Commun. 6, 7615. https://doi.org/10.1038/ncomms8615.

Halpern, B.S., Walbridge, S., Selkoe, K.A., 2008. A global map of human impact on marine ecosystems. Science 319, 946–948. https://doi.org/10.1126/science.1151084.

Holon, F., Marre, G., Parravicini, V., et al., 2018. A predictive model based on multiple coastal anthropogenic pressures explains the degradation status of a marine ecosystem: implications for management and conservation. Biol. Conserv. 222, 125–135. https://doi.org/10.1016/j.biocon.2018.04.006.

Holon, F., Mouquet, N., Boissery, P., et al., 2015. Fine-scale cartography of human impacts along French mediterranean coasts: a relevant map for the management of marine ecosystems. PLoS One 10, e0135473. https://doi.org/10.1371/journal.pone.0135473.

Houngnandan, F., Kéfi, S., Deter, J., 2020. Identifying key-conservation areas for Posidonia oceanica seagrass beds. Biol. Conserv. 247, 108546. https://doi.org/10.1016/j.biocon.2020.108546.

IMO, 2018. Automatic identification systems (AIS). https://www.imo.org/en/OurWork/Safety/Pages/AIS.aspx. (Accessed 19 October 2018). http://www.imo.org/en/ourwork/safety/navigation/pages/ais.aspx.

Intergovernmental Panel on Climate Change (IPCC), 2022. Changing Ocean, marine ecosystems, and dependent communities. In: The Ocean and Cryosphere in a Changing Climate: Special Report of the Intergovernmental Panel on Climate Change. Cambridge University Press, Cambridge, pp. 447–588.

Jialeng, G., Suárez de la Fuente, S., Smith, T., 2023. BoatNet: automated small boat composition detection using deep learning on satellite imagery. UCL Open Environ 5, e058. https://doi.org/10.14324/111.444/ucloe.000058.

Kanjir, U., Greidanus, H., Oštir, K., 2018. Vessel detection and classification from spaceborne optical images: a literature survey. Remote Sensing of Environment 207, 1–26. https://doi.org/10.1016/j.rse.2017.12.033.

LeCun, Y., Bengio, Y., Hinton, G., 2015. Deep learning. Nature 521, 436–444. https://doi.org/10.1038/nature14539.

March, D., Metcalfe, K., Tintoré, J., Godley, B.J., 2021. Tracking the global reduction of marine traffic during the COVID-19 pandemic. Nat. Commun. 12, 2415. https://doi.org/10.1038/s41467-021-22423-6.

Martínez, M.L., Intralawan, A., Vázquez, G., et al., 2007. The coasts of our world: ecological, economic and social importance. Ecol. Econ. 63, 254–272. https://doi.org/10.1016/j.ecolecon.2006.10.022.

MEDOBS, 2024. Medobs. https://medtrix.fr/portfolio_page/medobs/. (Accessed 28 November 2018).

Milazzo, M., Badalamenti, F., Ceccherelli, G., Chemello, R., 2004. Boat anchoring on Posidonia oceanica beds in a marine protected area (Italy, western Mediterranean): effect of anchor types in different anchoring stages. J. Exp. Mar. Biol. Ecol. 299, 51–62. https://doi.org/10.1016/j.jembe.2003.09.003.

Paolo, F., Kroodsma, D., Raynor, J., et al., 2024. Satellite mapping reveals extensive industrial activity at sea. Nature 625, 85–91. https://doi.org/10.1038/s41586-023-06825-8.

Pasqualini, V., Pergent-Martini, C., Pergent, G., 1999. Environmental impact identification along the Corsican coast (Mediterranean sea) using image processing. Aquat. Bot. 65, 311–320. https://doi.org/10.1016/S0304-3770(99)00048-0.

Patel, K., Bhatt, C., Mazzeo, P.L., 2022. Deep learning-based automatic detection of ships: an experimental study using satellite images. Journal of Imaging 8, 182. https://doi.org/10.3390/jimaging8070182.

Pergent-Martini, C., Monnier, B., Lehmann, L., et al., 2022. Major regression of Posidonia oceanica meadows in relation with recreational boat anchoring: a case study from Sant'Amanza bay. J. Sea Res. 188, 102258. https://doi.org/10.1016/j.seares.2022.102258.

Pita, I., Seguin, R., Shin, Y.-J., et al., 2022. SAR satellite imagery reveals the impact of the Covid-19 crisis on ship frequentation in the French mediterranean waters. Front. Mar. Sci. 9. https://doi.org/10.3389/fmars.2022.845419.

Rouanet, E., Astuch, P., Bonhomme, D., et al., 2013. EVIDENCE OF ANCHOR EFFECT IN A POSIDONIA OCEANICA SEAGRASS MEADOW UNDER LOW ANCHORING PRESSURE VIA A MULTI-CRITERIA GRID.

Schohn, T., Astruch, P., Rouanet, E., 2019. Innovative management tools to survey boat traffic and anchoring activities within a marine protected area. Planning, nature and ecosystem services. https://doi.org/10.6093/978-88-6887-054.6.

Serra-Sogas, N., O'Hara, P.D., Pearce, K., et al., 2021. Using aerial surveys to fill gaps in AIS vessel traffic data to inform threat assessments, vessel management and planning. Mar. Pol. 133, 104765. https://doi.org/10.1016/j.marpol.2021.104765.

Skalski, P., 2019. SkalskiP/make-sense.

Soubirane, J., 2019. Shaping the future of earth observation with pléiades neo. In: 2019 9th International Conference on Recent Advances in Space Technologies (RAST), pp. 399–401.

Toivonen, T., Heikinheimo, V., Fink, C., et al., 2019. Social media data for conservation science: a methodological overview. Biol. Conserv. 233, 298–315. https://doi.org/10.1016/j.biocon.2019.01.023.

UNEP/MAP, 2024. Biological diversity in the mediterranean. https://www.unep.org/unepmap/resources/factsheets/biological-diversity. (Accessed 8 February 2024).

Wu, X., Sahoo, D., Hoi, S.C.H., 2020. Recent advances in deep learning for object detection. Neurocomputing 396, 39–64. https://doi.org/10.1016/j.neucom.2020.01.085.